Journal of Molecular Structure 973 (2010) 130–135

Contents lists available at ScienceDirect

Journal of Molecular Structure

journal homepage: www.elsevier.com/locate/molstruc

Cobalt(II) complex with new terpyridine ligand: An ab initio geometry optimization investigation

Artur Ciesielski *, Adam Gorczyński, Piotr Jankowski, Maciej Kubicki, Violetta Patroniak

Faculty of Chemistry, Adam Mickiewicz University, Grunwaldzka 6, 60780 Poznań, Poland

ARTICLE INFO

Article history:
Received 12 January 2010
Received in revised form 22 March 2010
Accepted 22 March 2010
Available online 25 March 2010

Keywords:
Coordination chemistry
Cobalt(II)
DFT
Geometry optimization

ABSTRACT

Structural parameters of a complex formed between Co(II), and a terpyridine ligand were investigated using the unrestricted Becke three-parameter hybrid exchange functional combined with the Lee–Yang–Parr correlation functional (B3LYP) with the LANL2DZ, 6-31G(d,p), and 6-31G++(d,p) basis sets applied for geometry optimizations. The computations reveal that frequently used methods, which take into consideration primary and secondary interactions, can often be efficient in optimizing structural geometries of systems based on organic molecules and transition-metal ions.

1. Introduction

Coordination complexes of transition-metals are the subject of detailed investigation in coordination chemistry since a few decades. The use of homotopic N donor ligands and metal ions in self-assembly processes has attracted much attention for the design and synthesis of novel functional materials [1,2]. Recent applications range from the controlled deposition of grid-type [2 × 2] cobalt(II) complexes onto graphite into ordered supramolecular assemblies [3,4], to new electrochemical approach to detect target DNA molecules from solution based on catalytic oxidation of cobalt(II) complex containing 4,4′-di-*t*-butyl-2,2′-bipyridine [5]. Terpyridine ligand, i.e. polypyridyls derivative has been employed to generate many metallosupramolecular architectures such as helicates, grids, metal-chain oligo-pyridylamido systems, metallacycles [6]. Their applications include molecular machines [7–9], liquid crystals [10], catalysts for both organic and inorganic reactions [11–14], and as both therapeutic and imaging agents in medicine [15,16]. Of particular relevance to the above expectations is the accurate prediction of molecular geometries in the complex. The geometrical optimizations of the systems consisting of up to 50 atoms, is now a routine. A lot of experience has been collected using the performance of Hartree–Fock (HF) approaches and methods based on Møller–Plesset (MP) perturbation theory or density functional theory (DFT) These methods perform well within an expected accuracy of ±0.02 Å or better for bond lengths in the systems consisting of main group elements [17]. However, transition-metal (TM) compounds are more difficult to handle due to partially filled d shells, which render classical HF and MP approaches incapable of taking up the challenge, apart from special situations e.g. d^0 or d^{10} systems, or closed shell species with large gaps. Thus, bearing in mind the cost of more computationally demanding methods such as CCSD(T), we have chosen DFT as a suitable technique allowing us to perform geometry optimization at an affordable cost and acceptable accuracy. Bühl et al. carried out a thorough research where a number of density-functional/basis-set combinations was tested, including B3LYP, for their ability to reproduce the geometries of first [18], second [19] and third row [20] transition-metal complexes. It concluded that although a slight advantage of hybrid functionals like B3P86 or B3PW91 is noticeable, restricting ourselves to the selected few may be misleading as for the performance of each functional is not uniform and depends on the evaluated property and the nature of the system investigated. Among the plethora of existing functionals, B3LYP has been given particular attention especially over the past few years. In spite of its decreasing popularity in favour of more sophisticated density approximations, i.e. Hybrid Meta GGA (generalized gradient approximation) and Fully Non Local description, B3LYPs appliance is still being discussed in terms of general performance [21] and determination of complexes geometry and multiplicity to name a few [22]. Ramos et al. published an interesting review [21] concerning not only the general performance of density functionals, but also attempted to emphasize and compare the results obtained by the B3LYP functional with other well-established ones. The results varied from excellent to poor

* Corresponding author. Present address: ISIS/UMR CNRS 7006, Université de Strasbourg, 8 allée Gaspard Monge, 67000 Strasbourg, France.
E-mail address: ciesielski@unistra.fr (A. Ciesielski).

0022-2860/$ - see front matter © 2010 Elsevier B.V. All rights reserved.
doi:10.1016/j.molstruc.2010.03.057

depending on the property and the system under study, confirming at the same time that despite being outperformed in certain instances, for the other ones B3LYP may still compete with more elaborated basis sets. In this paper we investigate the molecular geometries of metal–ligand complex {[Co**L**Cl_2](CH_3CN)}, computed with the unrestricted B3LYP functional with the LANL2DZ, 6-31G(d), and 6-31G++(d,p) basis sets.

2. Experimental section

2.1. General

The metal salts were used without further purification as supplied from Aldrich. NMR spectrum was obtained with a Varian Gemini 300 MHz spectrometer and was calibrated against the residual protonated solvent signals ($CDCl_3$: δ = 7.24 ppm) which are given in ppm. Mass spectra were determined by using a Waters Micromass ZQ spectrometer. Sample solutions were introduced into the mass spectrometer source with a syringe pump at a flow rate of 40 μL min^{-1} with a capillary voltage of +3 kV and a desolvation temperature of 300 °C. Source temperature was 120 °C. The cone voltage (*Vc*) was set to 30 V to allow transmission of ions without fragmentation processes. Scanning was performed from *m*/*z* = 200 to 1000 for 6 s, and 10 scans were summed to obtain the final spectrum. Microanalyses were obtained by using a Perkin–Elmer 2400 CHN microanalyser. Mass FAB+ spectrum was determined by using ZAB-HF VG spectrometer in m-nitrobenzylalcohol matrix.

2.2. Preparation of **L**

To a mixture of 2-(6-methylpyridin-2-yl)-6-(trimethylstannyl)pyridine [23,24] (0.955 g, 2.9 mmol), 4,6-dichloro-2-phenylpyrimidine [25] (0.258 g, 1.15 mmol) and LiCl (0.31 g, 7.3 mmol) was gradually added degassed toluene (40 mL) and [$Pd(PPh_3)_4$] (0.065 g, 0.056 mmol) under an argon atmosphere. The reaction mixture was stirred and heated at reflux for 24 h, and then the toluene was evaporated under reduced pressure. The residue was purified by column chromatography on alumina (dichloromethane/hexane, 4:6) and 5% methanol in dichloromethane to afford (0.167 g, 34%) of compound **4** [26] and (90 mg, 22%) of ligand **L**. **5(L)**: ^{1}H NMR (300 MHz, $CDCl_3$, 25 °C): *d* = 8.68 (t, 1H, *J* = 7.5 Hz), 8.60 (m, 3H), 8.47 (s, 1H), 8.42 (d, 2H, *J* = 7.8 Hz), 8.04 (t, 1H, *J* = 7.8), 7.96 (t, 1H, *J* = 7.8), 7.56 (m, 3H), 2.67 (s, 3H). FAB–MS: *m*/*z* = 359.1 (M+, 10). $C_{21}H_{15}ClN_4$ (358.82) calcd. C = 70.29, H = 4.21, N = 15.61, found C = 70.21, H = 4.24, N = 15.99.

2.3. Preparation of Co(II) complex {[Co**L**Cl_2](CH_3CN)}

A mixture of $CoCl_2{\cdot}6H_2O$ (7 mg, 0.028 mmol) and **L** (47 mg, 0.028 mmol) in CH_3CN/CH_2Cl_2 (1:1, 4 mL) was stirred at room temperature for 48 h. Pink complex {[Co**L**Cl_2](CH_3CN)} was isolated in quantitative yield by evaporation of the solvent. ESI–MS: *m*/*z* = 467 (100%) [Co**L**Cl(H_2O)]$^+$, 359 (35%) [H**L**]$^+$. {[Co**L**Cl_2](CH_3CN)} (529.71) calcd. C = 52.15, H = 3.43, N = 13.22, found C = 52.21, H = 3.39, N = 13.26.

2.4. Calculation methods

The molecular geometries of complex {[Co**L**Cl_2](CH_3CN)} (Fig. 1) have been fully optimized using the unrestricted Becke three-parameter hybrid exchange functional combined with the Lee–Yang–Parr correlation functional (B3LYP) [27,28] which was used with the LANL2DZ [29], 6-31G(d,p), and 6-31G++(d,p) basis sets for geometry optimization. Calculations with these basis sets were are usually quite consistent with experimental results [22,30,31]. Gaussian 03 program [32], running on an SGI Altix 350 Linux server in 1 Itanium 2 processor at 1.5 GHz was used for calculations [33].

2.5. Crystal structure determination of complex {[Co**L**Cl_2](CH_3CN)}

Diffraction data were collected at 200(1)K by the ω-scan technique on a KUMA-KM4CCD diffractometer with graphite–monochromatized Mo Kα radiation (λ = 0.71073 Å). Data were corrected for Lorentz-polarization and absorption effects [34]. Accurate unit-cell parameters were determined by the least-squares fit of 3836 reflections of highest intensity, chosen from the whole experiment. The structure was solved with SIR-92 [35] and refined with the full-matrix least-squares procedure on F^2 by SHELXL97 [36] Scattering factors incorporated in SHELXL97 were used. Function $\sum w(|F_o|^2 - |F_c|^2)^2$ was minimized, with $w^{-1} = [\sigma^2(F_o)^2 + 0.013\,P^2]$, where *P* is $[\mathrm{Max}(F_o^2, 0) + 2F_c^2]/3$. All non-hydrogen atoms were refined anisotropically, the hydrogen atoms were placed geometrically, in idealized positions, and refined as rigid groups; U_{iso}'s of these hydrogen atoms were set as 1.2 (1.3 for methyl groups) times U_{eq}'s of the appropriate carrier atoms. Relevant crystal data are listed in Table 1, together with refinement details.

3. Results and discussion

Metal-catalysed coupling reactions of halopyridines and their derivatives are a long-established means of synthesis of polypyridines, including quaterpyridines, though milder and more selective procedures have been more recently developed [37–39]. In the present case, multidentate ligand **L** was obtained as a side product of a Stille coupling reaction [40], as outlined in Scheme 1. Furthermore, we also found another side product **4**; unfortunately the main reaction product **3** was not found, which is not surprising for such a kind of reaction [26].

Table 1
Experimental crystal data, data collection and structure refinement details.

Formula	$C_{21}H_{15}Cl_3CoN_4{\cdot}(CH_3CN)$
Formula weight	529.70
Crystal system	Triclinic
Space group	P-1
a (Å)	7.6694(4)
b (Å)	12.9089(6)
c (Å)	12.9769(7)
α (°)	65.591(5)
β (°)	76.513(4)
γ (°)	82.018(4)
V (Å^3)	1136.34(10)
Z	2
D_x (g cm^{-3})	1.55
F (0 0 0)	538
μ (mm^{-1})	1.13
Crystal size (mm)	0.3 × 0.15 × 0.03
Θ range (°)	2.73–28.01
h k l range	$-9 \leqslant h \leqslant 9$ $-16 \leqslant k \leqslant 16$ $-16 \leqslant l \leqslant 17$
Reflections	
Collected	9824
Unique (R_{int})	4965(0.037)
With $I > 2\sigma(I)$	2559
No. of parameters	291
$R(F)$ [$I > 2\sigma(I)$]	0.035
$wR(F^2)$ [$I > 2\sigma(I)$]	0.051
$R(F)$ [all data]	0.072
$wR(F^2)$ [all data]	0.055
Goodness of fit	0.93
max/min Δρ (e Å^{-3})	0.33/−0.41

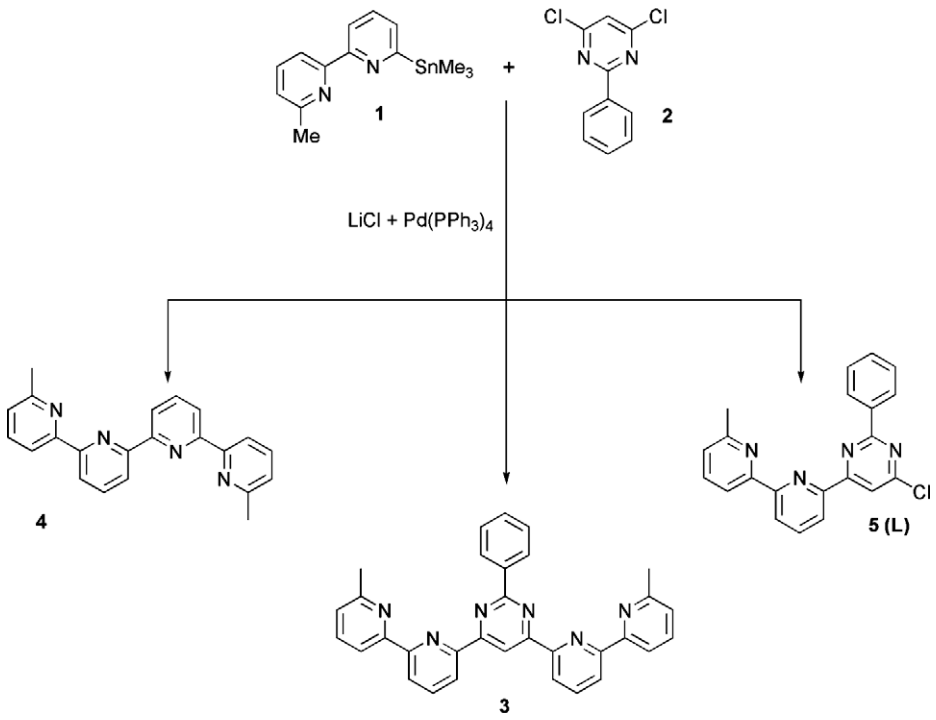

Scheme 1. Reaction scheme for the synthesis of ligand **L**.

An equimolar reaction of cobalt(II) chloride with ligand **L** provided a new complex. The complex was characterized with electrospray ionization mass spectrometry. The ESI–MS spectrum of complex showed the signals at $m/z = 467$ $[CoLCl(H_2O)]^+$, 359 $[HL]^+$ which means that in solution mononuclear species and ligand molecules occur.

3.1. Crystal data for complex {[Co**L**Cl_2](CH_3CN)}

The bipyridine fragment is almost planar, with the dihedral angle between the two rings of 2.38(9)°. The disposition of nitrogen atoms is *cis*, thus allowing to coordinate to the same Co atom, with typical Co–N distances of 2.154 Å and 2.040 Å. The pyrimidine ring is significantly twisted, by 27.3(1)°, with respect to the bipyridine plane. Nevertheless, the sense of the twist is such that the nitrogen atom in ortho-position, with respect to the ring junction, remains approximately coplanar with the plane of bipyridine and Co atom (Fig. 2). The Co–N14 distance, of 2.551(2) Å is outside the range of typical Co–N bonds. Interestingly, the contacts of this length are quite rare: in the Cambridge Crystallographic Database there are only 12 examples of intramolecular Co–N distances within the range 2.5–2.6 Å (excluding the Co···NO_3 contacts). This contact might be therefore regarded as the weak bond, and the Co atom will be 5-coordinated. The coordination can be described as deformed trigonal bipyramid (Fig. 3), with the nitrogen and Co atoms making the basal plane (maximum deviation of 0.050 Å) and Cl1 and Cl2 at its apexes (deviations from the basal plane of 1.683 Å and −2.157 Å, respectively). The terminal phenyl ring is inclined by 11.90(12)° with respect to the pyrimidine ring, and by 38.98(7)° to the opposite terminal pyridine ring. This last value can be the measure of the overall conformation of the ligand molecule. The crystal structure is determined mainly by van der Waals interactions and some weak intermolecular C–H···Cl and C–H···π interactions (Fig. 4, Table 2). The packing of complex molecules creates voids in the structure which are filled by acetonitrile molecules, which are also connected with the ligand by relatively short C–H···N contact.

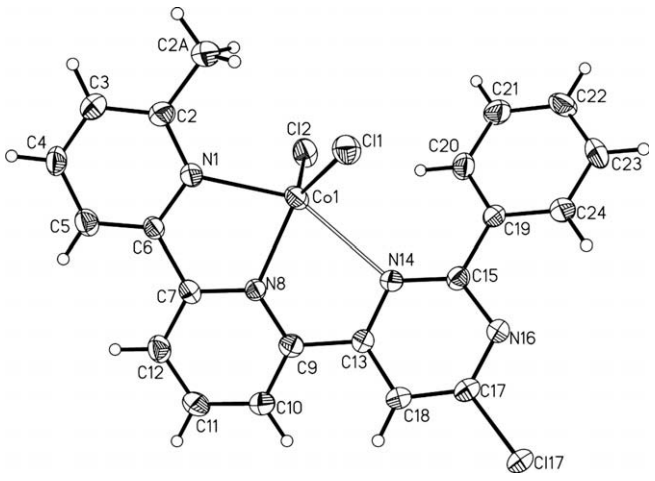

Fig. 1. Perspective view of one of the complex {[Co**L**Cl_2](CH_3CN)} together with the numbering scheme. The anisotropic displacement ellipsoids are drawn at 50% probability level, hydrogen atoms are depicted as spheres with arbitrary radii.

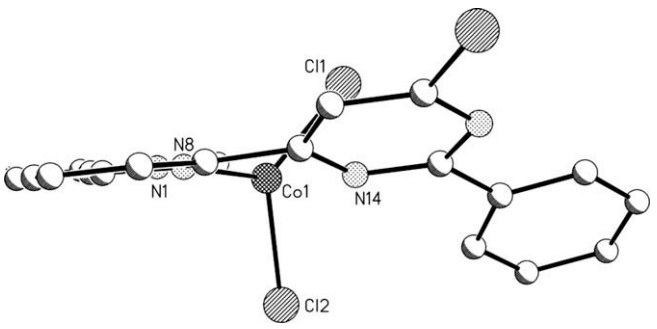

Fig. 2. Perspective of the N14 atom to the plane of bipyridine fragment in the crystal structure of the {[Co**L**Cl_2](CH_3CN)} complex.

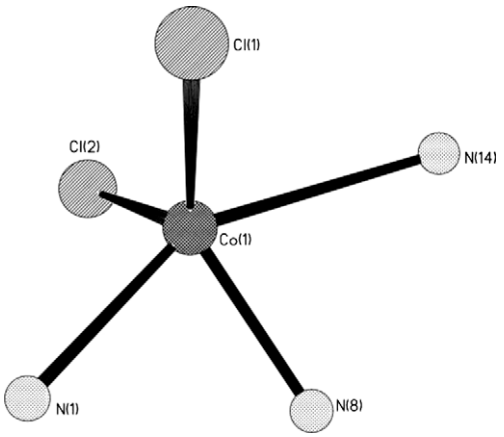

Fig. 3. The coordination of Co in the crystal structure of the {[Co**L**Cl_2](CH_3CN)} complex.

3.2. Calculations data

The effect of state must be taken under consideration with regard to geometry optimization of {[Co**L**Cl_2](CH_3CN)} complex. Solid state structures, which can be obtained from X-ray diffraction technique by measurement of the distances between regions of electron density, might simultaneously be distorted by the packing effects. In contrast, quantum calculations, which interpret the compound within the framework of fixed nuclei, presented in this paper correspond to the gas phase, hence we must realize that the results will vary to a certain extent as it is principally impossible to directly compare the results acquired from DFT and XRD-analysis. No polarizable continuum model (PCM) was used in order to account the effect of solvent as, contrary to the packing effects in solid, even in more complex and charged biological molecules such an effect may in general be neglected without making serious errors [41]. Table 3 summarizes key computed parameters of the {[Co**L**Cl_2](CH_3CN)} complex, which consist of the selected bond distances, angles between them as well as torsions. What is substantial, the calculations have been performed assuming that the Co(II) ion might exist in its doublet or in quadruplet state, what reflects the differences in the data acquired, especially the one concerning ions coordination sphere. It is generally considered that chlorine ions are classified as the low-field ligands. Furthermore, nitrogen donor atoms also relatively weakly split energetic levels of cobalts

Table 2
Experimental hydrogen bond data (Å, °; Cg1 describes the centroid of the phenyl ring).

D	H	A	D–H	H···A	D···A	D–H···A
C4	H4	Cl17[a]	0.95	2.86	3.561(2)	132
C12	H12	Cl2[b]	0.95	2.72	3.584(2)	151
C18	H18	N31[c]	0.95	2.42	3.338(3)	164
C33	H331	Cg4[d]	0.98	2.76	3.630(4)	148

Symmetry codes:
[a] $x, y, -1 + z$.
[b] $-x, 1 - y, -z$.
[c] $x, 1 + y, z$.
[d] $1 - x, -y, 1 - z$.

d orbitals. Taking into consideration these two factors the quadruplet state is more feasible to occur and this indeed is consonant with the experimental data. Theoretical calculations of the ground state of Co(II) complex revealed that, regardless of the basis set applied, quadruplet state is always more thermodynamically stable than the doublet state. The energetic difference deriving from the complexes' multiplicity expressed in kcal/mol is as follows: 9.92, 10.95 and 8.85 for 6-31G(d,p), 6-31G++(d,p) and LANL2DZ basis set, respectively. These results conform well with the hypothesis stated above.

For the quadruplet state, the values of Co1–N1 and Co1–N8 bond distances are well reproduced, with the smallest deviation for LANL2DZ basis set (+0.0156 Å) and underestimation of less than 0.01 Å (6-31G(d,p) and 6-31G++(d,p)) for Co1–N1 and Co1–N8, respectively. Calculations performed for the doublet state appeared to be largely underestimated; deviations within a range of 0.118–0.2 Å. Uniqueness of the Co1–N14 bond is obvious, as for values obtained with the use of B3LYP function are completely not in line with those obtained from the X-ray structural analysis. Nevertheless, deviations computed for quadruplet state are about half the value of doublet state, with the 6-31G(d,p) basis set being the least inaccurate of them all (0.2265 Å). As far as the Co1–Cl1 bond is concerned, the best estimates of these values are given by 6-31G(d,p)-quadruplet state and LANL2DZ doublet state (deviation of +0.045 Å and +0.047 Å, respectively). It is noteworthy that 6-31G(d,p) basis set-quadruplet state also compares well with the experimental values of Co1–Cl2 bond distance, the deviation being slightly greater than the former one (0.0557 Å) yet still about twice less than the remaining ones (errors in the range from 0.071 Å to 0.111 Å for Co1–Cl1 and from 0.0947 Å to 0.1367 Å for Co1–Cl2). Computational data concerning the remaining bond distances

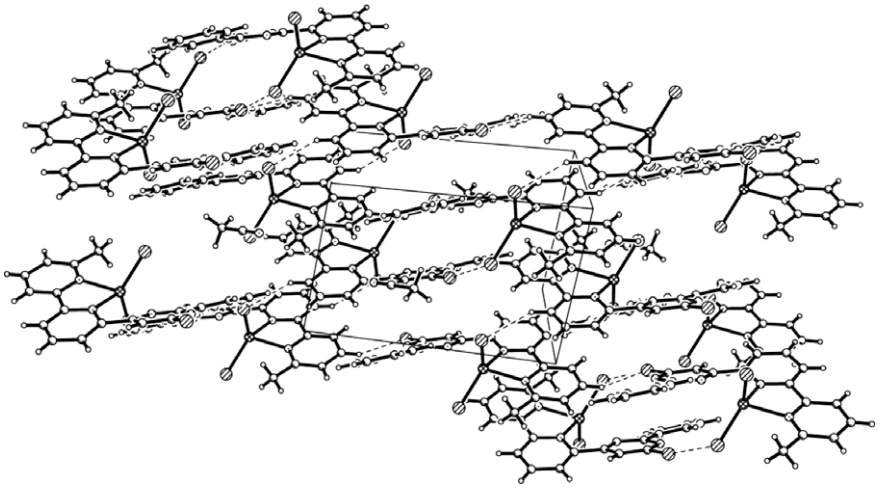

Fig. 4. Crystal packing of the {[Co**L**Cl_2](CH_3CN)} as seen approximately along [0 0 1] direction.

Table 3
Experimental and theoretical characterization of [Co**L**Cl2] (distances in Å, dihedral angles in degrees).

	Exp.	UB3LYP 6-31G(d,p) doublet state	UB3LYP 6-31G++(d,p) doublet state	UB3LYP LANL2DZ doublet state	UB3LYP 6-31G(d,p) quadruplet state	UB3LYP 6-31G++(d,p) quadruplet state	UB3LYP LANL2DZ quadruplet state
Co1–N1	2.1536(19)	1.975	1.956	1.953	2.181	2.179	2.138
Co1–Cl1	2.2329(7)	2.304	2.345	2.278	2.280	2.344	2.320
Co1–N14	2.5515(18)	1.999	1.990	1.989	2.325	2.275	2.184
N1–C2	1.346(3)	1.346	1.360	1.350	1.344	1.360	1.342
N8–C7	1.348(2)	1.338	1.350	1.345	1.347	1.355	1.338
N14–C13	1.355(2)	1.369	1.385	1.370	1.351	1.371	1.356
Co1–N8	2.0402(17)	1.922	1.920	1.882	2.032	2.043	2.004
Co1–Cl2	2.2583(7)	2.353	2.395	2.357	2.316	2.376	2.366
N1–C6	1.353(2)	1.366	1.378	1.366	1.350	1.365	1.354
N8–C9	1.347(3)	1.335	1.347	1.342	1.341	1.353	1.338
N14–C15	1.339(3)	1.354	1.372	1.360	1.355	1.370	1.344
Cl2–H(C20)	2.654(3)	2.505	2.441	2.422	2.447	2.464	2.368
N1–Co1–N8	78.28(7)	81.45	82.01	82.09	78.19	77.29	78.14
N1–Co1–Cl2	92.57(5)	89.30	88.78	88.76	92.09	87.62	89.22
N8–Co1–Cl1	126.19(5)	108.04	109.50	116.24	117.07	114.35	109.10
N8–Co1–N14	73.05(6)	81.71	82.48	82.30	75.84	77.85	79.43
Cl1–Co1–N14	88.31(4)	91.82	91.42	92.44	91.19	93.13	93.14
C2–N1–C6	118.8(2)	119.76	120.50	119.50	120.29	120.48	119.50
C13–N14–C15	116.44(18)	117.35	118.28	117.05	117.14	118.50	117.71
N1–C6–C7–N8	0.6(3)	1.99	2.05	2.94	8.99	2.82	2.40
N8–C9–C13–N14	−25.1(3)	−2.73	−4.09	−4.42	−16.37	−12.37	−5.88
N14–C15–C19–C20	−11.7(4)	−46.28	−33.39	−38.04	−26.69	−25.44	−32.93
N1–Co1–Cl1	105.95(6)	92.25	92.50	93.38	97.56	94.27	92.62
N1–Co1–N14	151.08(6)	163.12	164.43	164.34	153.80	154.95	157.51
N8–Co1–Cl2	111.56(6)	97.93	96.66	98.38	103.74	104.02	97.91
Cl1–Co1–Cl2	121.56(3)	153.93	153.74	145.28	139.15	141.05	152.73
Cl2–Co1–N14	101.28(5)	94.19	94.33	94.70	97.33	101.38	95.48
C7–N8–C9	119.73(18)	123.06	124.01	122.50	121.27	122.44	122.90
C15–N16–C17	116.40(19)	118.21	119.31	118.78	118.10	118.63	117.59

listed in Table 3 are in good agreement with each other, regardless of the basis set applied. In general, their average deviation does not exceed 0.02 Å, with Cl2–H(C20) distance as an exception since DFT calculations, as seen above, not necessarily need to apply perfectly to the systems containing halogen complexes [37]. From these data it is apparent that performed quadruplet state calculations are in far greater consonance with corresponding X-ray crystallographic data than the doublet ones, with the 6-31G(d,p) being the most accurate among them. The same tendency might be observed for the bond angles, i.e. the best results are found for 6-31G(d,p) where the maximum estimation error does not exceed 2.88° excluding the following angles: N8–Co1–Cl1, N8–Co1–Cl2, Cl2–Co–N14, Cl1–Co–Cl2. First three are underestimated for 9.13°, 7.93° and 3.96°, respectively, while the positive deviation of the latter one exceeds 17°. Nevertheless we must remember that lack of an appropriate description of the dispersion effect in DFT approaches might result in such deviations, which are even greater for other basis sets presented and B3LYP functional in general while considering halides. Furthermore, such inaccuracies are a consequence of the marked above effect of state of the complex under study and the fact that DFT approaches parameterize molecules geometry in the framework of fixed nuclei, not electron density. Such incomplete electron–nuclear distribution description is even more visible while considering dihedral angles, which did not appear to be well comparative. Torsion coordinates take up large place in molecular space at the same time having volumes relative to those of electron densities within those vibrational elements, hence the errors. The so far most exact basis set largely deviated from the N1–C6–C7–N8 value, the deviation being about four times larger than others. The remaining data also include relatively high errors, albeit the data most approximate to experimental N8–C9–C13–N14 and N14–C15–C19–C20 values are performed by both 6-31G(d,p) and 6-31G++(d,p) basis sets. Therefore, considering and summarizing whole acquired data, 6-31G(d,p) basis set is recommended for computational study of presented complex when using DFT functionals.

4. Conclusions

We report the synthesis of a new terpyridine ligand **L** and its Co(II) complex, which may be of interest in several fields of cobalt coordination chemistry such as catalysis, crystal engineering and (molecular) electronics [42,43].

The present study shows that DFT calculations can be used as an additional tool to investigate the molecular geometries of transition-metal complexes with good accuracy. Results of our research show that by performing calculations with the unrestricted B3LYP functional and applying the 6-31G(d,p) basis set with the polarizable continuum model of theory we are very close to predict the real structure of metal–ligand complex molecule. One must note that the largest deviations, regardless of the basis set applied, appeared to concern not only the unusual Co–N14 bond which is however outside the range of typical Co–N bonds, but also angles and torsions. The inaccuracies arise from limitations of fixed-nuclear theory in quantum chemistry, as for we have performed comparison between gas phase optimized geometry and the solid state structure obtained from X-ray diffraction analysis. Theoretical calculations of the ground state of the complex evaluated proved that what we face is Co(II) in its quadruplet state. It is also noteworthy that such calculations let us easily determine the multiplicity of the complexated metal ion and thus foresee its magnetic properties what is, as mentioned above, crucial in establishment of the compounds potential applications.

5. Supplementary material

Crystallographic data (excluding structure factors) have been deposited with the Cambridge Crystallographic Data Centre, No.

CCDC-725563. Copies of these may be obtained, free of charge, from: The Director, CCDC, 12 Union Road, Cambridge CB2 1EZ, UK. Fax: +44 1223 336 033, e-mail:deposit@ccdc.cam.ac.uk, or www: www.ccdc.cam.ac.uk.

Acknowledgments

A.C. thanks Prof. Paolo Samorì for fruitful discussions and the French Ministry of Research for a predoctoral fellowship. This research was carried out as part of the Polish Ministry of Higher Education and Science project (Grant No. NN 204 2716 33).

References

[1] M.J. Hannon, L.J. Childs, Supramol. Chem. 16 (2004) 7–22.
[2] K.H. Thompson, C. Orvig, Dalton Trans. (2006) 761–764.
[3] M.S. Alam, S. Strömsdörfer, V. Dremov, P. Müller, J. Kortus, M. Ruben, J.-M. Lehn, Angew. Chem. Int. Ed. 44 (2005) 7896–7900.
[4] G. Pace, A.R. Stefankiewicz, J.M. Harrowfield, J.-M. Lehn, P. Samorì, ChemPhysChem 10 (2009) 699–705.
[5] D. Xue, C.M. Elliott, P. Gong, D.W. Grainger, C.A. Bignozzi, S. Caramori, J. Am. Chem. Soc. 129 (2007) 1854–1855.
[6] C.R.K. Glasson, L.F. Lindoy, G.V. Meehan, Coordin. Chem. Rev. 252 (2008) 940–963.
[7] E.R. Kay, D.A. Leigh, F. Zerbetto, Angew. Chem. Int. Ed. 46 (2007) 72–191.
[8] T.A.V. Khuong, J.E. Nuñez, C.E. Godinez, M.A. Garcia-Garibay, Accounts Chem. Res. 39 (2006) 413.
[9] V. Ferri, M. Elbing, G. Pace, M.D. Dickey, M. Zharnikov, P. Samorì, M. Mayor, M.A. Rampi, Angew. Chem. Int. Ed. 47 (2008) 3407–3409.
[10] C. Tschierske, Angew. Chem. Int. Ed. 39 (2000) 2454–2458.
[11] F. Vögtle, F. Alfter, Supramolecular Chemistry, Wiley, New York, 1991.
[12] M.L. Merlau, M. del Pilar, M. SonBinh, T. Nguyen, J.T. Hupp, Angew. Chem. Int. Ed. 40 (2001) 4239–4242.
[13] O. Ohmori, M. Fujita, Chem. Commun. (2004) 1586–1587.
[14] C.T. Yeung, H.L. Yeung, C.S. Tsang, W.Y. Wong, H.L. Kwong, Chem. Commun. (2007) 5203–5205.
[15] A.C.G. Hotze, B.M. Kariuki, M.J. Hannon, Angew. Chem. Int. Ed. 45 (2006) 4839–4842.
[16] C.D.B. Vandevyver, A.S. Chauvin, S. Comby, J.C.G. Bünzli, Chem. Commun. (2007) 1716–1718.
[17] W. Koch, M.C. Holthausen, A Chemist's Guide to Density Functional Theory, Wiley-VCH, New York, 2001.
[18] M. Bühl, H. Kabrede, J. Chem. Theor. Comput. 2 (2006) 1282–1290.
[19] M.P. Waller, H. Braun, N. Hojdis, M. Bühl, J. Chem. Theor. Comput. 3 (2007) 2234–2242.
[20] M. Bühl, C. Reimann, D.A. Pantazis, T. Bredow, F. Neese, J. Chem. Theor. Comput. 4 (2008) 1449–1459.
[21] S.F. Sousa, P.A. Fernandes, M.J. Ramos, J. Phys. Chem. A 111 (2007) 10439–10452.
[22] I. Iwakura, T. Ikeno, T. Yamada, Angew. Chem. Int. Ed. 44 (2005) 2524–2527.
[23] P. Jutzi, U. Gilge, J. Organomet. Chem. 246 (1983) 163–168.
[24] G.V. Long, S.E. Boyd, M.M. Harding, I.E. Buys, T.W. Hambley, J. Chem. Soc., Dalton Trans. (1993) 3175–3180.
[25] K. Burdeska, H. Fuhrer, G. Kabas, A.E. Siegrist, Helv. Chim. Acta 64 (1981) 113–152.
[26] A.R. Stefankiewicz, M. Wałęsa, P. Jankowski, A. Ciesielski, V. Patroniak, M. Kubicki, Z. Hnatejko, J.M. Harrowfield, J.-M. Lehn, Eur. J. Inorg. Chem. (2008) 2910–2920.
[27] A.D. Becke, J. Chem. Phys. 98 (1993) 5648–5652.
[28] C.T. Lee, W.T. Yang, R.G. Parr, Phys. Rev. B 37 (1988) 785–789.
[29] P.J. Hay, W.R. Wadt, J. Chem. Phys. 82 (1985) 299–310.
[30] T. Ikeno, I. Iwakura, S. Yabushita, T. Yamada, Org. Lett. 4 (2002) 517–520.
[31] I. Iwakura, T. Ikeno, T. Yamada, Org. Lett. 6 (2004) 949–952.
[32] R.C. Gaussian 03, M.J. Frisch, G.W. Trucks, H.B. Schlegel, G.E. Scuseria, M.A. Robb, J.R. Cheeseman, J.J.A. Montgomery, T. Vreven, K.N. Kudin, J.C. Burant, J.M. Millam, S.S. Iyengar, J. Tomasi, V. Barone, B. Mennucci, M. Cossi, G. Scalmani, N. Rega, G.A. Petersson, H. Nakatsuji, M. Hada, M. Ehara, K. Toyota, R. Fukuda, J. Hasegawa, M. Ishida, T. Nakajima, Y. Honda, O. Kitao, H. Nakai, M. Klene, X. Li, J.E. Knox, H.P. Hratchian, J.B. Cross, V. Bakken, C. Adamo, J. Jaramillo, R. Gomperts, R.E. Stratmann, O. Yazyev, A.J. Austin, R. Cammi, C. Pomelli, J.W. Ochterski, P.Y. Ayala, K. Morokuma, G.A. Voth, P. Salvador, J.J. Dannenberg, V.G. Zakrzewski, S. Dapprich, A.D. Daniels, M.C. Strain, O. Farkas, D.K. Malick, A.D. Rabuck, K. Raghavachari, J.B. Foresman, J.V. Ortiz, Q. Cui, A.G. Baboul, S. Clifford, J. Cioslowski, B.B. Stefanov, G. Liu, A. Liashenko, P. Piskorz, I. Komaromi, R.L. Martin, D.J. Fox, T. Keith, M.A. Al-Laham, C.Y. Peng, A. Nanayakkara, M. Challacombe, P.M.W. Gill, B. Johnson, W. Chen, M.W. Wong, C. Gonzalez, J.A. Pople, In Gaussian, Inc. Wallingford CT, 2004.
[33] <http://www-curri.u-strasbg.fr/>.
[34] O. Diffraction, Oxford Diffraction Ltd., Abingdon, England, 2007.
[35] A. Altomare, G. Cascarano, C. Giacovazzo, A. Guagliardi, J. Appl. Crystallogr. 26 (1993) 343–350.
[36] G.M. Sheldrick, Acta Crystallogr. Sect. A 64 (2008) 112–122.
[37] U.S. Schubert, H. Hofmeier, G.R. Newkome, Modern Terpyridine Chemistry, Wiley-VCH, 2006.
[38] E.C. Constable, M.J. Hannon, P. Harverson, M. Neuburger, D.R. Smith, V.F. Wanner, L.A. Whall, M. Zehnder, Polyhedron 19 (2000) 23–34.
[39] D.B.D. Amico, F. Calderazzo, M. Curiardi, L. Labella, F. Marchetti, Inorg. Chem. 43 (2004) 5459–5465.
[40] J.K. Stille, Angew. Chem. Int. Ed. 25 (1986) 508–523.
[41] S.F. Sousa, P.A. Fernandes, M.J. Ramos, J. Phys. Chem. A 113 (2009) 14231–14236.
[42] P.J. Low, Dalton Trans. (2005) 2821–2824.
[43] Y. Sato, Y. Nakayama, H. Yasuda, J. Organomet. Chem. 689 (2004) 744–750.